

# FNDC5 and AKR1B10 inhibit the proliferation and metastasis of adrenocortical carcinoma cells by regulating AMPK/mTOR pathway

DANYAN CHEN<sup>1</sup>, RONGXI HUANG<sup>1</sup>, FANG REN<sup>2</sup>, HONGMAN WANG<sup>1</sup>, CHENGJIAN WANG<sup>1</sup> and YU ZHANG<sup>1</sup>

Departments of <sup>1</sup>Endocrinology and <sup>2</sup>Emergency, Chongqing General Hospital,  
University of Chinese Academy of Sciences, Chongqing 401147, P.R. China

Received September 16, 2022; Accepted January 24, 2023

DOI: 10.3892/etm.2023.11835

**Abstract.** Being a rare malignancy, adrenocortical carcinoma (ACC) exhibits aggressiveness and poor prognosis. Fibronectin type III domain-containing protein 5 (FNDC5) is a transmembrane protein involved in multiple types of cancer. Aldo-keto reductase family 1 member B10 (AKR1B10) has a suppressive role in ACC. The present study aimed to investigate the role of FNDC5 in ACC cells as well as its mechanisms related to AKR1B10. The Gene Expression Profiling Interactive Analysis database predicted FNDC5 expression in tumour tissue of patients suffering from ACC and the overall survival rate. Western blotting as well as reverse transcription-quantitative PCR were used for the examination of the transfection efficiency of FNDC5-overexpression vector (Oe-FNDC5) and small interfering (si)RNA against AKR1B10. Cell Counting Kit-8 was employed for the assessment of cell viability. The proliferation, migration and invasion of the transfected cells were assessed by 5-ethynyl-2'-deoxyuridine staining, wound healing and Transwell assays. Additionally, cell apoptosis was evaluated by flow cytometry and caspase-3 activity was determined by ELISA. The levels of epithelial-mesenchymal transition- and 5'-AMP-activated protein kinase (AMPK)/mTOR signalling pathway-associated proteins were assessed by western blotting. The interaction between FNDC5 and AKR1B10 was confirmed by co-immunoprecipitation. FNDC5 levels in ACC tissue were reduced compared with normal tissue. After over-expressing FNDC5, proliferation, migration and invasion of NCI-H295R cells were suppressed, while cell apoptosis was promoted. FNDC5 interacted with AKR1B10 and AKR1B10

knockdown promoted proliferation, migration and invasion while inhibiting the apoptosis of NCI-H295R cells transfected with si-AKR1B10. The AMPK/mTOR signalling pathway was activated by FNDC5 overexpression, which was subsequently suppressed by AKR1B10 knockdown. Collectively, FNDC5 overexpression inhibited proliferation, migration and invasion while promoting apoptosis of NCI-H295R cells via triggering the AMPK/mTOR signalling pathway. These effects were counteracted by AKR1B10 knockdown.

## Introduction

Being a rare malignancy, adrenocortical carcinoma (ACC) exhibits aggressiveness as well as a poor prognosis. A number of patients present local invasion or metastasis at the time of the diagnosis (1). The annual ACC incidence is 0.7-2.0 cases in every 1 million individuals, accounting for 0.2% of cancer deaths in the Netherlands (2). According to the staging criteria of the Union for International Cancer Control and the American Joint Committee on Cancer (3), R0 resection can be achieved in stage I or II with an ideal prognosis. However, for stage III or IV resection the 5-year survival rate is low, reported to be 6-15% (4,5). Therefore, it is particularly important to identify molecular markers for the study of ACC pathogenesis and auxiliary clinical treatment.

Aldo-keto reductase family 1 member B10 (AKR1B10), which belongs to the AKR superfamily, consists of 316 amino acids and its gene is located on chromosome 7q33 (6). AKR1B10 stimulation suppresses ACC cell proliferation and promotes apoptosis (7). BioGRID (8) predicted a potential interaction between fibronectin type III domain-containing protein 5 (FNDC5) and AKR1B10. A transmembrane protein, FNDC5 is also a prohormone that is released from irisin (9). FNDC5 expression is elevated in ovarian cancer tissue and suppresses epithelial ovarian cancer cell proliferation, migration and invasion (10). Irisin induces G<sub>2</sub>/M cell cycle arrest and suppresses proliferation and invasion of glioblastoma cells (11). FNDC5 expression is reduced in non-small cell lung cancer cells (NSCLCs) cells and increases the sensitivity of NSCLC cells to paclitaxel (12). Irisin/FNDC5 suppress the viability, invasion and migration as well as epithelial-mesenchymal transition (EMT) of osteosarcoma cells (13). Irisin also induces G<sub>1</sub> arrest

*Correspondence to:* Dr Danyan Chen, Department of Endocrinology, Chongqing General Hospital, University of Chinese Academy of Sciences, 118 Xingguang Avenue, Liangjiang New Area, Chongqing 401147, P.R. China  
E-mail: Chendanyan\_123@163.com

**Key words:** fibronectin type III domain-containing protein 5, aldo-keto reductase family 1 member B10, adrenocortical carcinoma, AMPK/mTOR pathway

and inhibits proliferation and migration of pancreatic cancer cells via the 5'-AMP-activated protein kinase (AMPK)/mTOR signalling pathway (14). Nevertheless, to the best of our knowledge, the role of FNDC5 in ACC remains unclear.

The present study aimed to explore the role of FNDC5 in the proliferation, migration, invasion and EMT of ACC cells and the underlying mechanisms.

## Materials and methods

**Bioinformatics.** Gene Expression Profiling Interactive Analysis (GEPIA) database analyzed the expression of FNDC5 in the tumour tissue of patients with ACC and the correlation between FNDC5 and AKR1B10. Encyclopedia of RNA Interactomes database predicted the correlation between FNDC5 expression and the overall survival in patients with ACC.

**Cell culture and transfection.** ACC cell line (NCI-H295R) provided by BeNa Culture Collection was cultivated in DMEM (Gibco; Thermo Fisher Scientific, Inc.) which was supplemented with 10% FBS (Beyotime Institute of Biotechnology) and 1% penicillin/streptomycin (Beyotime Institute of Biotechnology) at 37°C with 5% CO<sub>2</sub>.

Full-length cDNA of human FNDC5 was cloned into the pcDNA3.1 vector (Thermo Fisher Scientific, Inc.) to generate an FNDC5 overexpression vector (Oe-FNDC5). A pcDNA3.1 empty vector was used as the negative control (Oe-NC). Small interfering (si)RNAs specific for AKR1B10 (si-AKR1B10#1, 5'-CAGGATATCGGCACATTGACTGG-3' and si-AKR1B10#2, GGCCTATGTCTATCAGAATGAAC) as well as its si-NC (5'-AAGACAUUGUGUGUCCGCCCTT-3') were constructed by Guangzhou RiboBio Co., Ltd. NCI-H295R cells in logarithmic growth phase were seeded in 6-well plates (1x10<sup>6</sup> cells/well) and cultured until the cell confluence reached 80%. A total of 20 µg Oe-FNDC5, Oe-NC, si-AKR1B10 and si-NC was transfected into NCI-H295R cells separately using Lipofectamine 3000 reagent (Thermo Fisher Scientific, Inc.) and incubated for 6 h at 37°C. At 48 h post-transfection, the collection of cells was implemented for ensuing experiments.

**Reverse transcription-quantitative polymerase chain reaction (RT-qPCR).** RT of RNA, which was isolated from NCI-H295R cells utilizing TRIzol<sup>®</sup> reagent (Thermo Fisher Scientific, Inc.) according to the manufacturer's instructions, into cDNA was performed using the PrimeScript Reverse Transcriptase kit (Takara Bio, Inc.), according to the manufacturer's protocol. qPCR was performed using the SYBR<sup>®</sup> PremixEX Taq<sup>™</sup> kit (Takara Bio, Inc.). The qPCR thermocycling conditions were as follows: Initial denaturation at 95°C for 10 min; followed by 40 cycles of 95°C for 15 sec and 64°C for 30 sec. FNDC5 and AKR1B10 mRNA levels were quantified using the 2<sup>-ΔΔC<sub>q</sub></sup> method and normalized to the internal reference gene (15). The following primer pairs (Sangon Biotech) were used for qPCR: FNDC5 forward, 5'-CCGCCAGTATGACAT CATTGAA-3' and reverse, 5'-GTCACCTCACACCACTCA GG-3'; AKR1B10 forward, 5'-CATGAAGTGGGGGAAGCC AT-3' and reverse, 5'-CGTTACAGGCCCTCCAGTTT-3'; and GAPDH forward, 5'-GGAGCGAGATCCCTCCAAAAT-3' and reverse, 5'-GGCTGTTGTCATACTTCTCATGG-3'.

**Western blot analysis.** Total protein was isolated from NCI-H295R cells utilizing RIPA buffer (Beyotime Institute of Biotechnology) and quantified using a BCA Protein assay kit (Beyotime Institute of Biotechnology). Total protein (30 µg/lane) was separated by SDS-PAGE on 5-10% gels and transferred onto a PVDF membrane. The membranes were blocked with 5% BSA (Thermo Fisher Scientific, Inc.) for 1.5 h at room temperature and incubated overnight with primary antibodies against FNDC5 (cat. no. ab174833; 1:1,000), E-cadherin (cat. no. ab40772; 1/1,000), N-cadherin (cat. no. ab76011; 1/5,000), Snail (cat. no. ab216347; 1/1,000), AKR1B10 (cat. no. ab192865; 1/1,000), phosphorylated (p)-AMPK (cat. no. ab133448; 1/1,000), AMPK (cat. no. ab207442; 1/1,000), p-mTOR (cat. no. ab109268; 1/1,000), mTOR (cat. no. ab134903; 1/10,000) and GAPDH (cat. no. ab9485; 1/2,500) from Abcam at 4°C. Subsequently, the membranes were incubated with a secondary anti-rabbit horseradish peroxidase-conjugated antibody (cat. no. ab6721; 1/2,000; Abcam) for 2 h at room temperature. The protein bands were visualized using BeyoECL Plus (Beyotime Institute of Biotechnology) and ImageJ software 1.8.0 (National Institutes of Health) was used for analysis of band intensity with GAPDH as the loading control.

**Cell Counting Kit-8 (CCK-8) assay.** Following transfection, NCI-H295R cells (2x10<sup>4</sup> cells/well) were plated into 96-well plates and incubated for 24, 48 and 72 h at 37°C. Afterwards, 10 µl CCK-8 solution (Beyotime Institute of Biotechnology) was added to each well for 2 h. The optical density at 450 nm was measured with a microplate reader.

**5-ethynyl-2'-deoxyuridine (EdU) incorporation assay.** Following transfection, NCI-H295R cells (2x10<sup>4</sup> cells/well) were seeded into 96-well plates and incubated with 20 µM EdU for 2 h at room temperature and DNA was stained using 10 µmol/l DAPI for 10 min at room temperature. The observation of cell proliferative capability was performed utilizing an inverted fluorescence microscope (magnification, x200). Green cells were the EdU/DAPI-positive cells.

**Wound healing assay.** Transfected NCI-H295R cells were seeded into 6-well plates at 1x10<sup>5</sup> cells/well and when cell confluency reached 90%, a wound was made using a 10-µl pipette tip and the remaining cells were cultured in serum-free DMEM (Gibco; Thermo Fisher Scientific, Inc.) at 37°C. Under an inverted light microscope (magnification, x100), the wounds were observed at 0 and 24 h. ImageJ software version 1.8.0 (National Institutes of Health) was used for the determination of cell migration rate. The migration rate was calculated as follows: (Wound width at 0 h-wound width at 24 h)/wound width at 0 h x100%.

**Transwell assay.** A total of 1x10<sup>5</sup> transfected NCI-H295R cells were plated in the upper chambers of Transwell plates that were pre-coated with Matrigel at 37°C for 1 h. Serum-free DMEM (Gibco; Thermo Fisher Scientific, Inc.) was added into the top chambers while the bottom chambers were filled with 800 µl DMEM containing 10% FBS. Following 48 h incubation at 37°C, the migratory cells were exposed for 10 min to 4% paraformaldehyde fixation at room temperature as well as

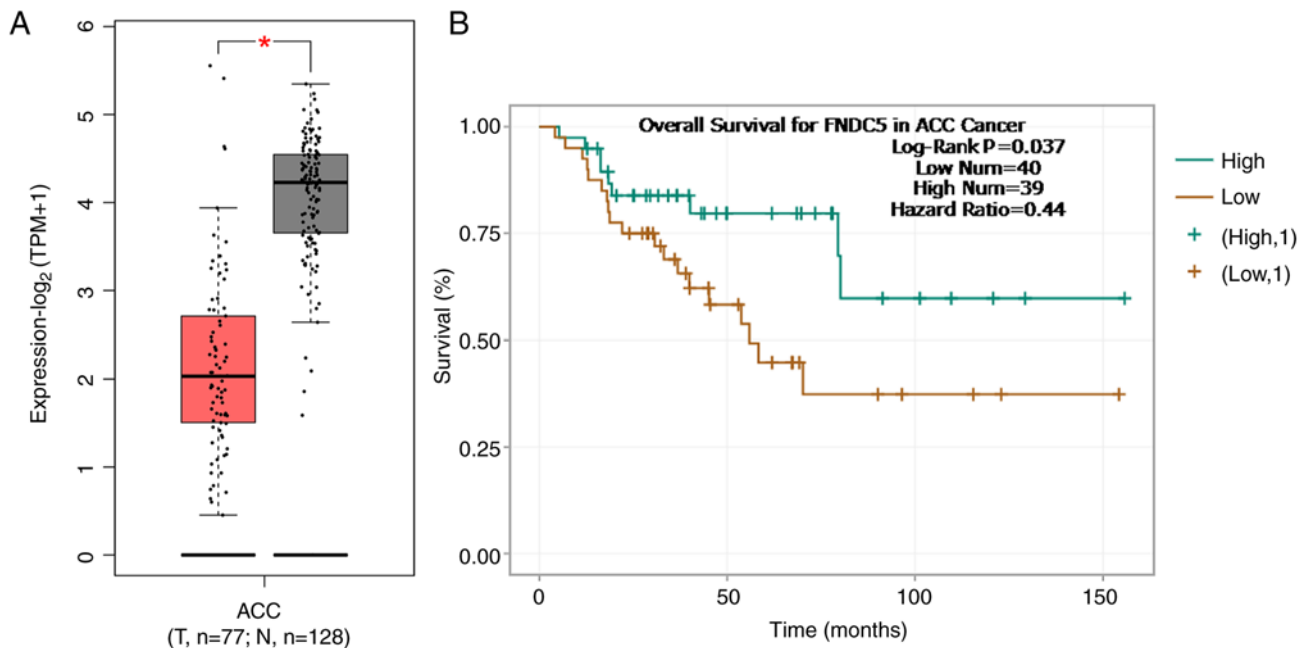


Figure 1. FNDC5 is lowly expressed in ACC and is associated with poor prognosis. (A) Expression of FNDC5 in ACC tissue was predicted by Gene Expression Profiling Interactive Analysis database. \* $P < 0.05$ . (B) Association between FNDC5 expression and overall survival was predicted by The Encyclopedia of RNA Interactomes database. FNDC5, fibronectin type III domain-containing protein 5; T, tumor; N, normal; ACC, adrenocortical carcinoma; TPM, transcripts per million.

10 min of 0.4% crystal violet staining at room temperature. Migratory cells were observed utilizing an inverted light microscope (magnification, x100).

**Cell apoptosis analysis.** Following plasmid transfection for 48 h, the transfected HL-60 cells ( $1 \times 10^6$ ) were washed with PBS and resuspended in 500  $\mu\text{l}$  binding buffer. Afterwards, the solution was transferred to a flow cytometry tube and mixed with 5  $\mu\text{l}$  Annexin V-fluorescein isothiocyanate staining solution (BD Biosciences). Cells were treated with 10  $\mu\text{l}$  propidium iodide solution (50  $\mu\text{g}/\text{ml}$ ; Dojindo Laboratories, Inc.) for 30 min at room temperature in the dark. The percentages of apoptotic cells were quantitated using a FACSCalibur flow cytometer (BD Biosciences) and FlowJo software (version 7.0; Tree Star, Inc.). The apoptosis rate was determined by calculating the percentage of early and late apoptotic cells.

**Measurement of caspase-3 activity.** Following centrifugation at 20,000  $\times g$  for 15 min at 4°C, activity of caspase-3 in cell supernatants was assessed using the Caspase-3 Colorimetric Assay kit (Abcam), according to the manufacturer's instructions. The optical density at 400 nm was measured with a microplate reader (Molecular Devices, LLC).

**Co-immunoprecipitation.** Following transfection, NCI-H295R cells were lysed with RIPA lysis buffer (Beyotime Institute of Biotechnology) and the supernatant was collected by centrifugation at 13,000  $\times g$  for 10 min at 4°C. 500  $\mu\text{g}$  cell lysate was incubated with antibodies against 2  $\mu\text{g}$  AKR1B10 (cat. no. NBP1-44998; Novus Biologicals), PDIA6 (cat. no. ab227545; Abcam) or IgG (cat. no. ab172730; Abcam) at 4°C overnight. Then, 50  $\mu\text{g}$  protein A magnetic beads were added

for capturing the complexes of AKR1B10 and PDIA6. After the IP reaction, 50  $\mu\text{g}$  protein G/A agarose beads were centrifuged at 1,000  $\times g$  for 3 min at 4°C to the bottom of the tube. The supernatant was then carefully absorbed, and the agarose beads were washed three times with 1 ml lysis buffer. A total of 15  $\mu\text{l}$  2X SDS sample buffer was finally added for boiling at 100°C for 5 min. Afterwards, the collected complexes were subjected to western blot analysis. The input was regarded as the positive control; IgG was the negative control.

**Statistical analysis.** Data from three independent replicates are presented as the mean  $\pm$  standard deviation. GraphPad Prism software (version 8.0.1; GraphPad Software, Inc.) was used for statistical analysis. Comparisons between multiple groups were performed using one-way ANOVA followed by Tukey's test.  $P < 0.05$  was considered to indicate a statistically significant difference.

## Results

**FNDC5 is lowly expressed in ACC and is associated with poor prognosis.** GEPIA database showed that the expression of FNDC5 was lower in the tumour tissue of patients with ACC than that in normal tissues (Fig. 1A). Encyclopedia of RNA Interactomes database indicated that low expression of FNDC5 was significantly associated with poor overall survival in patients with ACC (Fig. 1B).

**Overexpression of FNDC5 inhibits proliferation of ACC cells.** After transfecting Oe-FNDC5 into NCI-H295R cells, FNDC5 expression was significantly increased (Fig. 2A and B). Moreover, the viability and proliferation of NCI-H295R cells decreased following FNDC5 overexpression (Fig. 2C and D).

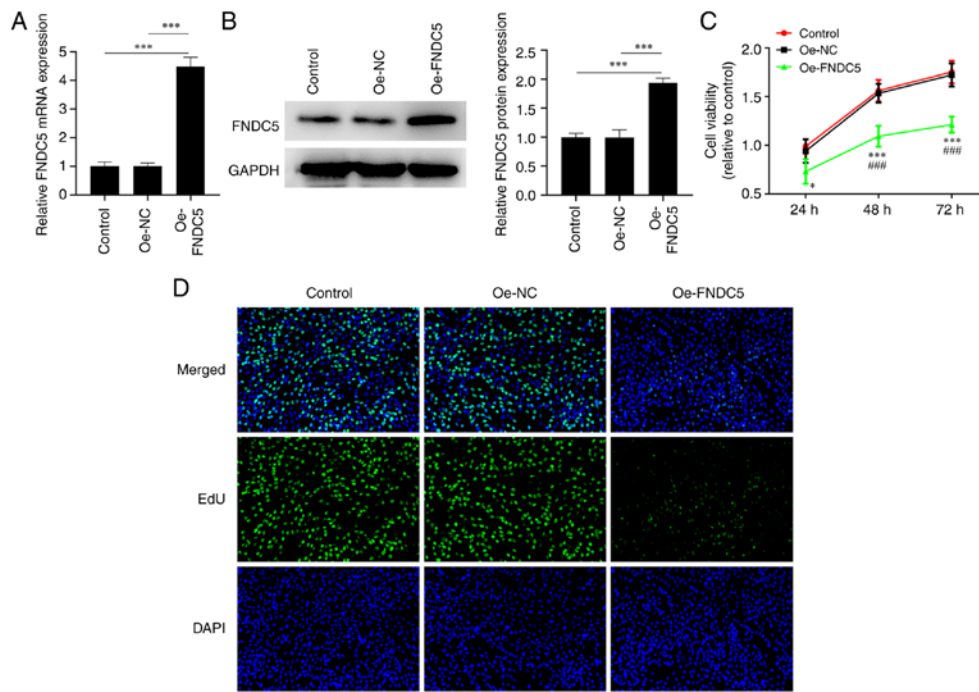


Figure 2. Overexpression of FNDC5 inhibits proliferation of ACC cells. The expression of FNDC5 in NCI-H295R cells was detected by (A) reverse transcription-quantitative PCR and (B) western blotting. \*\*\* $P < 0.001$ . (C) Viability of NCI-H295R cells transfected with Oe-FNDC5 was detected by Cell Counting Kit-8 assay. (D) Proliferation of NCI-H295R cells transfected with Oe-FNDC5 was detected by EdU staining. Magnification,  $\times 200$ . \* $P < 0.05$  and \*\*\* $P < 0.001$  vs. Control. ### $P < 0.001$  vs. Oe-NC. EdU, 5-ethynyl-2'-deoxyuridine; FNDC5, fibronectin type III domain-containing protein 5; Oe-NC, overexpression negative control.

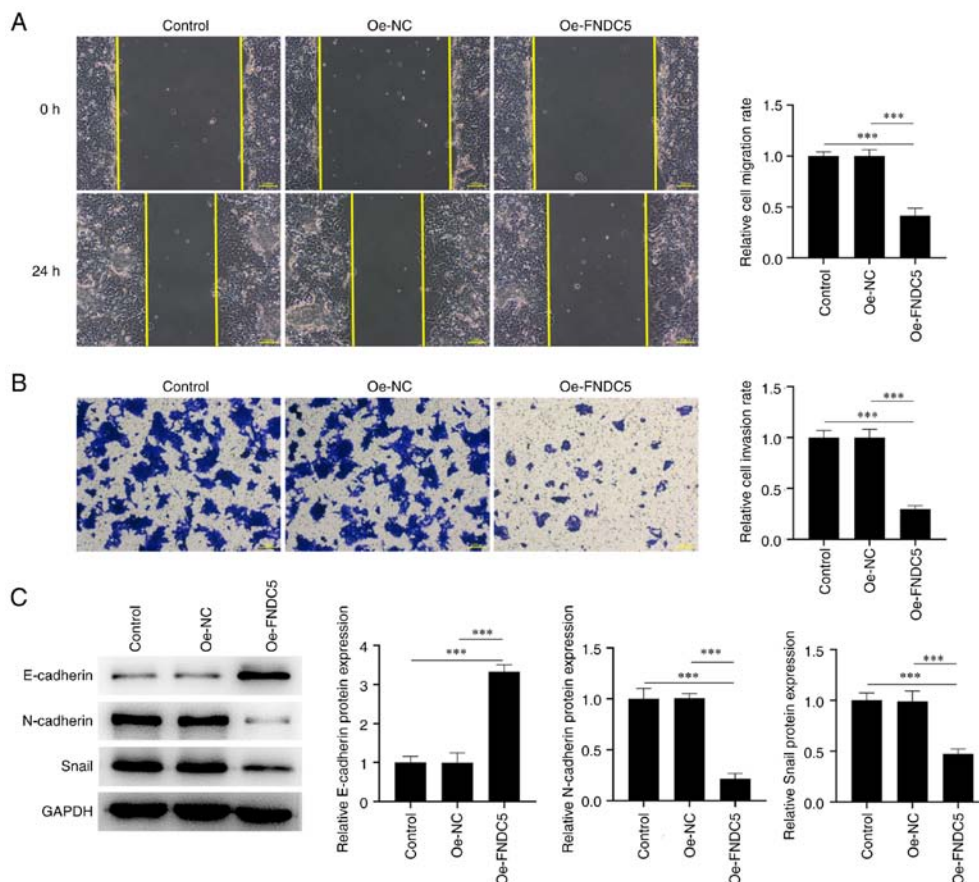


Figure 3. Overexpression of FNDC5 inhibits invasion, migration and EMT of adrenocortical carcinoma cells. (A) Migration and (B) invasion of NCI-H295R cells transfected with Oe-FNDC5 was detected by wound healing and Transwell assays (scale bar,  $100 \mu\text{m}$ ; magnification,  $\times 100$ ). (C) Expression of proteins associated with EMT in NCI-H295R cells transfected with Oe-FNDC5 was determined by western blotting. \*\*\* $P < 0.001$ . FNDC5, fibronectin type III domain-containing protein 5; Oe-NC, overexpression negative control.

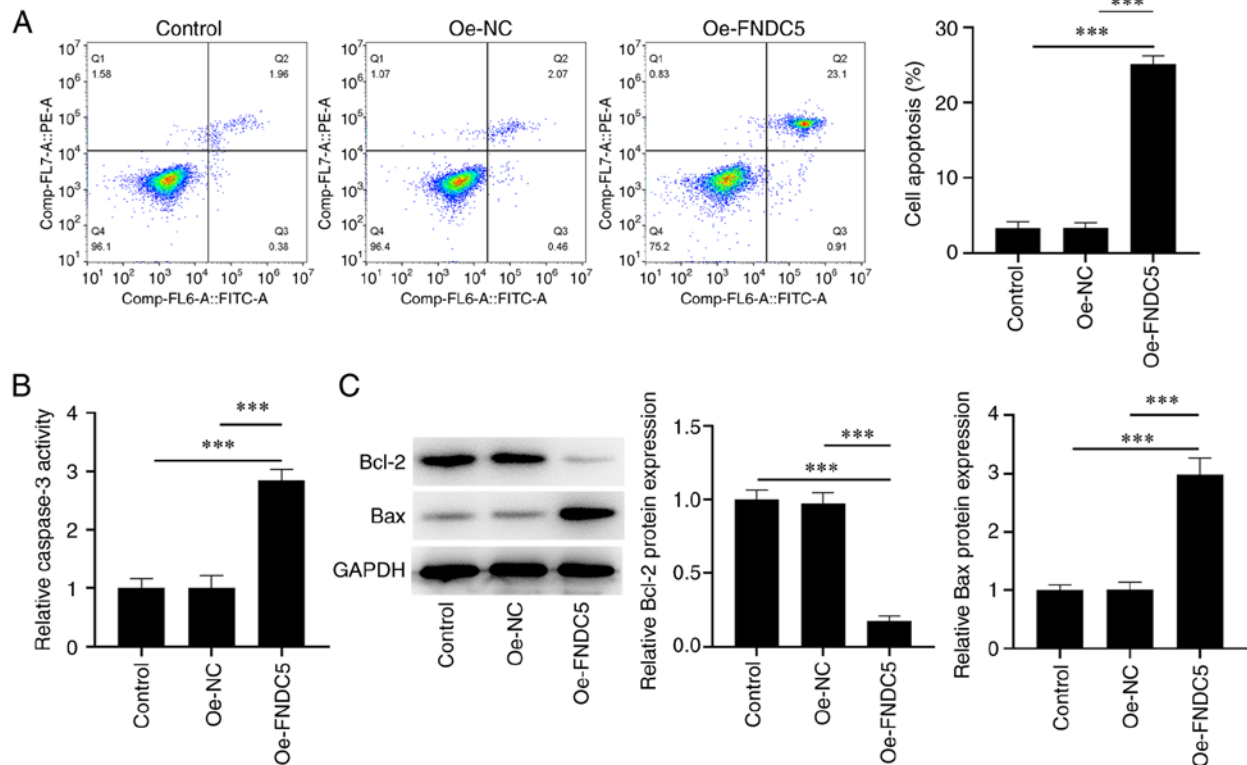


Figure 4. Overexpression of FNDC5 promotes apoptosis of adrenocortical carcinoma cells. (A) Apoptosis of NCI-H295R cells transfected with Oe-FNDC5 was measured utilizing a flow cytometer. (B) Caspase-3 activity was evaluated using an ELISA kit. (C) Expression of Bcl-2 and Bax in NCI-H295R cells transfected with Oe-FNDC5 was determined by western blotting. \*\*\*P<0.001. FNDC5, fibronectin type III domain-containing protein 5; Oe-NC, overexpression negative control.

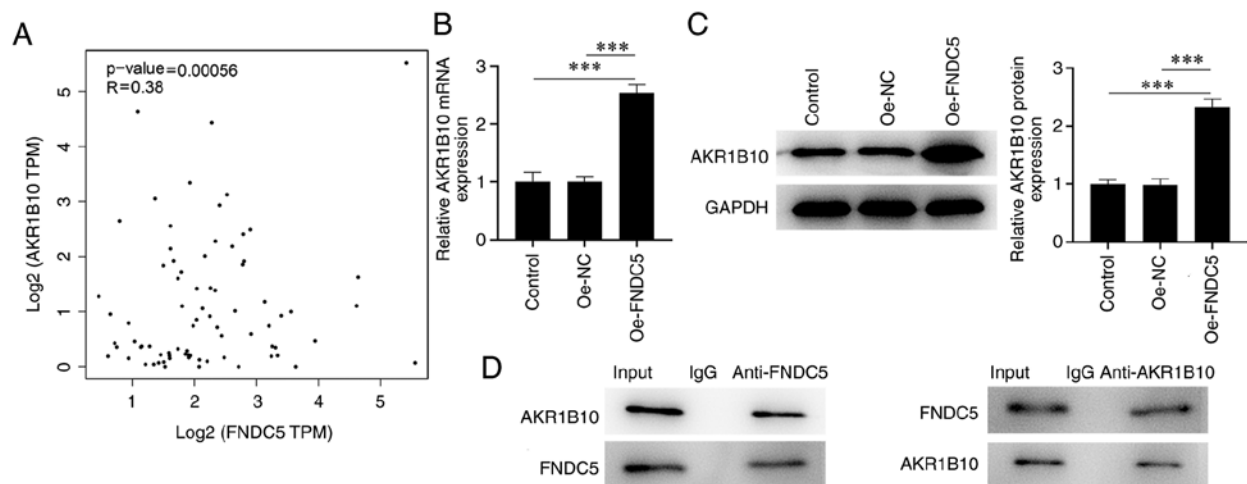


Figure 5. FNDC5 interacts with AKR1B10 in ACC cells. (A) Correlation between FNDC5 and AKR1B10 in ACC tissue was predicted by the Gene Expression Profiling Interactive Analysis database. Expression of AKR1B10 in NCI-H295R cells transfected with Oe-FNDC5 was detected by (B) reverse transcription-quantitative PCR and (C) western blot. (D) Interaction between FNDC5 and AKR1B10 in NCI-H295R cells was determined by co-immunoprecipitation. \*\*\*P<0.001. AKR1B10, aldo-keto reductase family 1 member B10; FNDC5, fibronectin type III domain-containing protein 5; Oe-NC, overexpression negative control; TPM, transcripts per million.

**Overexpression of FNDC5 inhibits invasion, migration and EMT of ACC cells.** The NCI-H295R cell invasion and migration were decreased after overexpressing FNDC5 (Fig. 3A and B). The expression levels of EMT-associated proteins showed that FNDC5 overexpression significantly promoted the expression of E-cadherin while inhibiting the expression of N-cadherin and Snail in NCI-H295R cells (Fig. 3C).

**Overexpression of FNDC5 promotes apoptosis of ACC cells.** Compared with the control and Oe-NC group, the proportion of apoptotic HL-60 cells was significantly increased following FNDC5 overexpression (Fig. 4A). Consistently, FNDC5 overexpression also increased caspase-3 activity (Fig. 4B). Bcl-2 expression was decreased in the Oe-FNDC5 group while the Bax expression was increased (Fig. 4C).



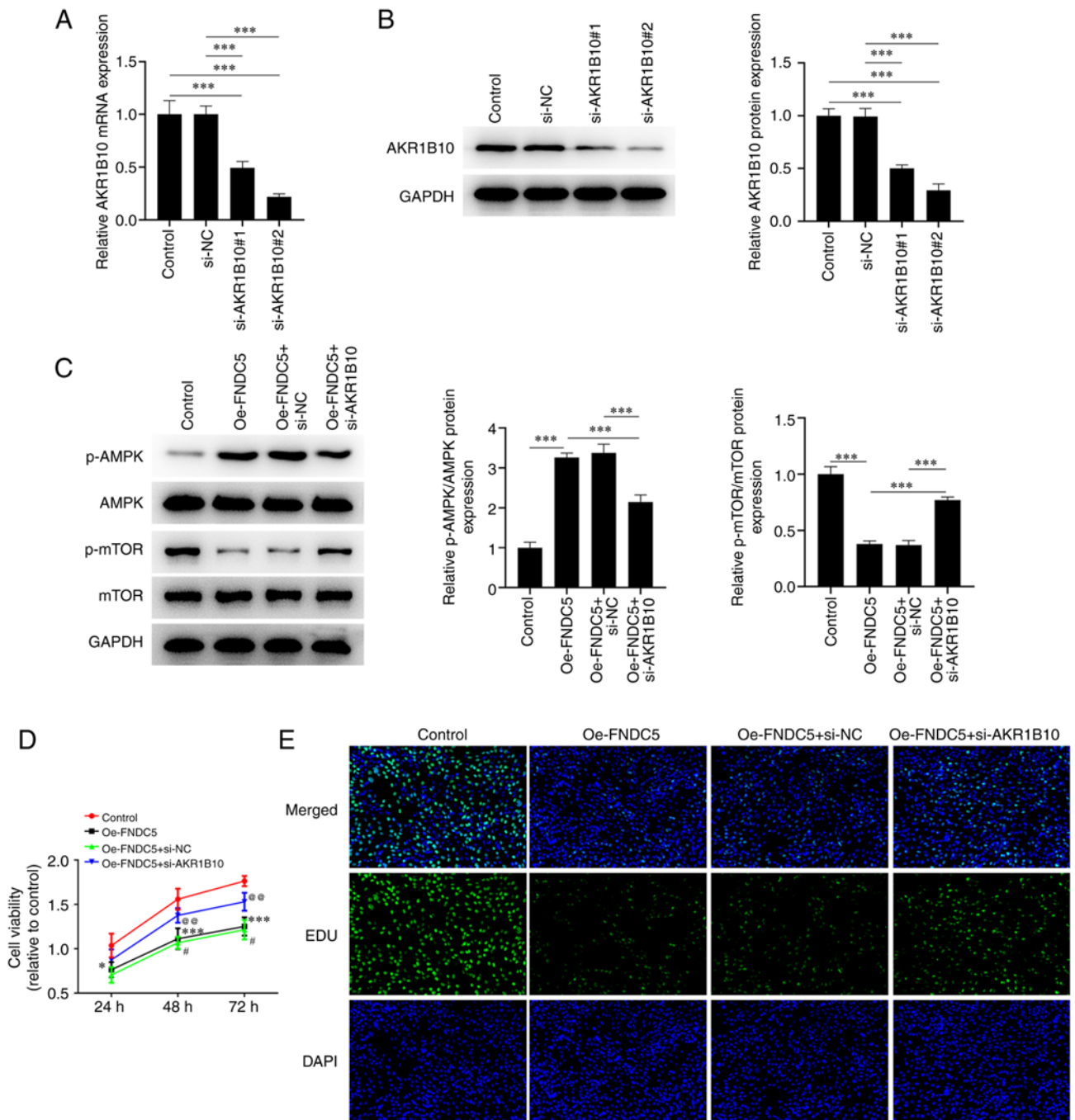


Figure 6. Downregulation of AKR1B10 reverses the effect of FNDC5 overexpression on proliferation of adrenocortical carcinoma cells by modulating the AMPK/mTOR pathway. The expression of AKR1B10 in NCI-H295R cells transfected with si-AKR1B10#1 or AKR1B10#2 was detected by (A) reverse transcription-quantitative PCR and (B) western blotting. (C) Expression of proteins associated with the AMPK/mTOR signalling pathway was detected by western blot. \*\*\* $P < 0.001$ . (D) Viability of NCI-H295R cells transfected with Oe-FNDC5 and si-AKR1B10 was detected by Cell Counting Kit-8 assay. (E) Proliferation of NCI-H295R cells transfected with Oe-FNDC5 and si-AKR1B10 was detected by EdU staining. Magnification, x200. \* $P < 0.05$  and \*\*\* $P < 0.001$  vs. Control. # $P < 0.05$  vs. Oe-FNDC5. @ $P < 0.01$  vs. Oe-FNDC5 + si-NC. AKR1B10, aldo-keto reductase family 1 member B10; AMPK, 5'-AMP-activated protein kinase; si-NC, small interfering negative control; FNDC5, fibronectin type III domain-containing protein 5; Oe, overexpression; EdU, 5-ethynyl-2'-deoxyuridine; p, phosphorylated.

**FNDC5 interacts with AKR1B10 in ACC cells.** GEPIA database indicated that FNDC5 had a positive correlation with AKR1B10 expression in patients with ACC (Fig. 5A). After overexpressing FNDC5, AKR1B10 expression in NCI-H295R cells increased (Fig. 5B and C). The expression of AKR1B10 was measured by incubation with anti-FNDC5 and expression of FNDC5 was analyzed by incubation with anti-AKR1B10, which indicated that FNDC5 interacted with AKR1B10 (Fig. 5D).

**Downregulation of AKR1B10 reverses the effect of FNDC5 overexpression on ACC cells by modulating the AMPK/mTOR pathway.** Following transfection with si-AKR1B10#1 or si-AKR1B10#2, AKR1B10 expression in NCI-H295R cells was decreased and was lower in the si-AKR1B10#2 group (Fig. 6A and B). Therefore, si-AKR1B10#2 transfection was used for subsequent experiments. FNDC5 overexpression increased the p-AMPK expression levels but decreased

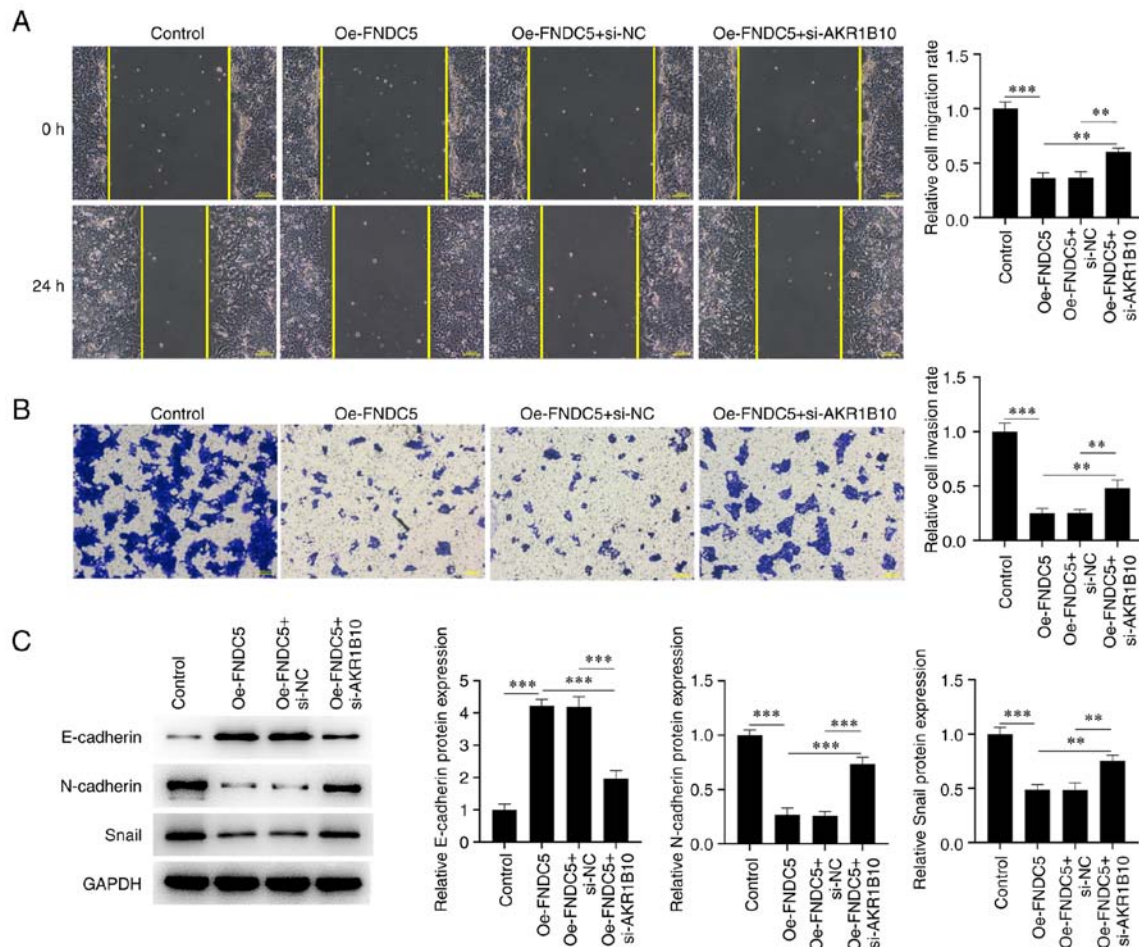


Figure 7. Downregulation of AKR1B10 reverses the effect of FNDC5 overexpression on migration and invasion of adrenocortical carcinoma cells by modulating the AMPK/mTOR pathway. (A) Migration and (B) invasion of NCI-H295R cells transfected with Oe-FNDC5 and si-AKR1B10 were detected by wound healing and Transwell assay. Scale bar, 100  $\mu$ m. Magnification, x100. (C) Western blotting was employed to detect expression of proteins associated with EMT. \*\* $P$ <0.01 and \*\*\* $P$ <0.001. AKR1B10, aldo-keto reductase family 1 member B10; AMPK, 5'-AMP-activated protein kinase; si-NC, small interfering negative control; FNDC5, fibronectin type III domain-containing protein 5; Oe, overexpression; Snail, Zinc finger protein SNAI1.

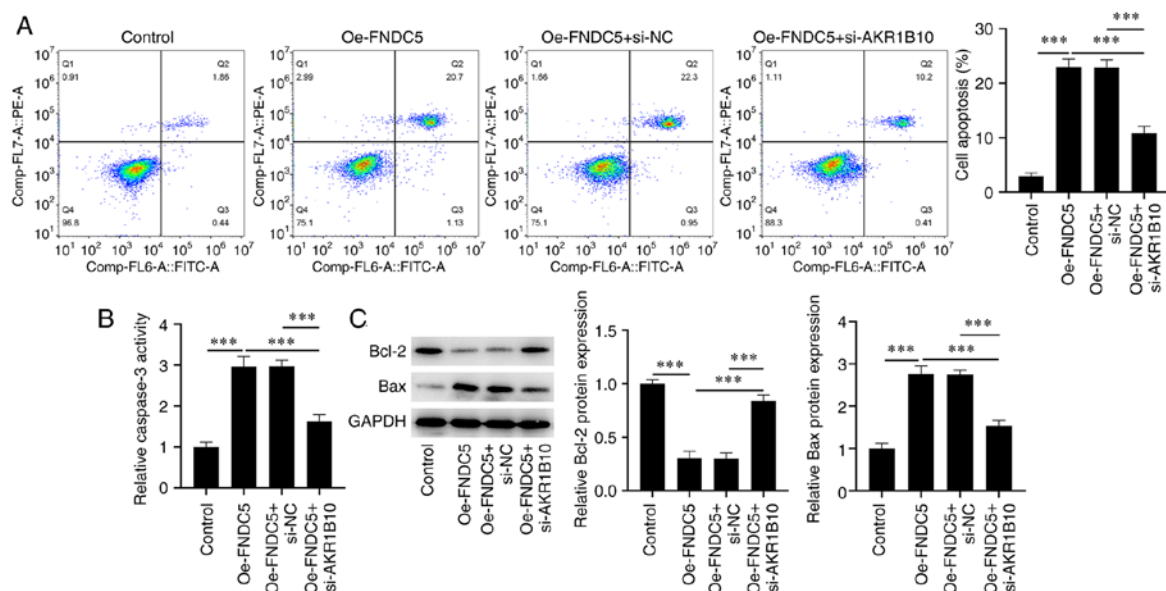


Figure 8. Downregulation of AKR1B10 reverses the effect of FNDC5 overexpression on apoptosis of adrenocortical carcinoma cells by modulating the AMPK/mTOR pathway. (A) Apoptosis of NCI-H295R cells transfected with Oe-FNDC5 was measured utilizing a flow cytometer. (B) Caspase-3 activity was tested by ELISA. (C) Expression of Bcl-2 and Bax in NCI-H295R cells transfected with Oe-FNDC5 was determined by western blot. \*\*\* $P$ <0.001. AKR1B10, aldo-keto reductase family 1 member B10; AMPK, 5'-AMP-activated protein kinase; si-NC, small interfering negative control; FNDC5, fibronectin type III domain-containing protein 5; Oe, overexpression.

expression of p-mTOR (Fig. 6C); these effects were then counteracted by AKR1B10 silencing. AKR1B10 silencing improved the decreased viability and proliferation of NCI-H295R cells caused by FNDC5 overexpression (Fig. 6D and E). Cell migration and invasion were also increased in NCI-H295R cells co-transfected with siAKR1B10#2 and Oe-FNDC5 (Oe-FNDC5 + si-AKR1B10 group) compared with Oe-FNDC5 + si-NC group (Fig. 7A and B). Moreover, expression of E-cadherin was downregulated while expression of N-cadherin and Snail was upregulated in the Oe-FNDC5 + si-AKR1B10 compared with Oe-FNDC5 + si-NC group (Fig. 7C). By contrast, the proportion of apoptotic NCI-H295R cells was decreased by AKR1B10 silencing compared with the Oe-FNDC5 + si-NC group (Fig. 8A). Western blot analysis indicated that AKR1B10 silencing in NCI-H295R cells transfected with Oe-FNDC5 increased Bcl-2 expression but decreased Bax expression and caspase-3 activity (Fig. 8B and C).

## Discussion

Irisin, which is proteolyzed by FNDC5, can convert white adipose tissue to brown, thus exerting its regulatory impacts on metabolic disease (16). It was discovered that FNDC5 is associated with the occurrence as well as the advancement of tumors. Compared with normal tissue, irisin expression in esophageal, gastric, colon and breast cancer is notably increased (17,18). At the same time, irisin may have a suppressive impact on proliferation, migration and invasion of breast and lung cancer, as well as osteosarcoma and other cells (19-21). The aforementioned studies demonstrated that irisin may be involved in the development of tumors. FNDC5 is highly expressed in renal (22), colorectal (23) and breast cancer (24). FNDC5 expression is increased in sorafenib-resistant hepatocellular carcinoma (HCC) cells and knockdown of FNDC5 enhances levels of ferroptosis in sorafenib-resistant HCC cells (25). In the present study, GEPIA database were used to analyze FNDC5 expression in ACC; FNDC5 expression was decreased in tumour tissues from patients with ACC. The present study demonstrated that FNDC5 may have suppressive effects on the proliferation, invasion and migration of NCI-H295R cells as well as EMT. Additionally, FNDC5 promoted apoptosis of NCI-H295R cells.

AKR1B10 is also reported to be involved in the development of multiple cancers (26,27). AKR1B10 expression is reduced in gastric cancer tissues and AKR1B10 suppresses the proliferation, migration and EMT of gastric cancer cells (26). AKR1B10 is decreased in colorectal cancer tissue and AKR1B10 knockdown facilitates proliferation and migration of colorectal cancer cells (27). AKR1B10 suppresses cell viability and colony formation while facilitating apoptosis of NCI-H295R cells (7). In the present study, the knockdown of AKR1B10 weakened the effect of FNDC5 overexpression on proliferation, invasion, migration, EMT and apoptosis of NCI-H295R cells.

AMPK/mTOR signalling pathway is a key regulator in a variety of tumors (28,29). A previous study discovered that frankincense, pine needle and geranium essential oil regulate the AMPK/mTOR pathway to inhibit proliferation of breast cancer cells (28). AMPK activator OSU-53 activates AMPK and regulates mTOR and its downstream signalling pathways to inhibit proliferation and viability of thyroid cancer cells (29). The combination of metformin and aspirin significantly

inhibits AMPK/STAT3-dependent phosphorylation of mTOR, reduce the expression of myeloid cell leukaemia-1 and Bcl-2 and suppresses proliferation, migration and invasion of pancreatic adenocarcinoma (30). In the present study, FNDC5 overexpression activated the AMPK/mTOR signalling pathway to suppress proliferation, invasion, migration and EMT but promote the apoptosis of NCI-H295R cells; these effects were counteracted by AKR1B10 knockdown.

The present study only investigated and discussed the effects and regulatory mechanisms of FNDC5 and AKR1B1 in ACC cells. Further *in vivo* tumour model experiments and validation of clinical tissue samples should be performed in future investigations to support the findings of the present study.

In conclusion, FNDC5 positively regulated AKR1B10 expression to inhibit the proliferation, invasion and migration of NCI-H295R cells by activating the AMPK/mTOR pathway.

## Acknowledgements

Not applicable.

## Funding

No funding was received.

## Availability of data and materials

The datasets used and/or analyzed during the current study are available from the corresponding author on reasonable request.

## Authors' contributions

DC designed and conceived the study and wrote the manuscript. DC, RH, FR and HW performed the experiments. CW and YZ analyzed data. All authors have read and approved the final manuscript. DC and RH confirm the authenticity of all the raw data.

## Ethics approval and consent to participate

Not applicable.

## Patient consent for publication

Not applicable.

## Competing interests

The authors declare that they have no competing interests.

## References

1. Vaidya A, Nehs M and Kilbridge K: Treatment of adrenocortical carcinoma. *Surg Pathol Clin* 12: 997-1006, 2019.
2. Kerkhofs TM, Verhoeven RH, Van der Zwan JM, Dieleman J, Kerstens MN, Links TP, Van de Poll-Franse LV and Haak HR: Adrenocortical carcinoma: A population-based study on incidence and survival in the Netherlands since 1993. *Eur J Cancer* 49: 2579-2586, 2013.
3. Edge SB and Compton CC: The American joint committee on cancer: The 7th edition of the AJCC cancer staging manual and the future of TNM. *Ann Surg Oncol* 17: 1471-1474, 2010.



4. Fassnacht M, Dekkers OM, Else T, Baudin E, Berruti A, de Krijger R, Haak HR, Mihai R, Assie G and Terzolo M: European society of endocrinology clinical practice guidelines on the management of adrenocortical carcinoma in adults, in collaboration with the European network for the study of adrenal tumors. *Eur J Endocrinol* 179: G1-G46, 2018.
5. Kiesewetter B, Riss P, Scheuba C, Mazal P, Kretschmer-Chott E, Haug A and Raderer M: Management of adrenocortical carcinoma: are we making progress? *Ther Adv Med Oncol* 13: 17588359211038409, 2021.
6. Giménez-Dejor J, Weber S, Fernández-Pardo Á, Möller G, Adamski J, Porté S, Parés X and Farrés J: Engineering aldo-keto reductase 1B10 to mimic the distinct 1B15 topology and specificity towards inhibitors and substrates, including retinoids and steroids. *Chem Biol Interact* 307: 186-194, 2019.
7. Chen D, Shen Z, Cheng X, Wang Q, Zhou J, Ren F, Sun Y, Wang H and Huang R: Homeobox A5 activates p53 pathway to inhibit proliferation and promote apoptosis of adrenocortical carcinoma cells by inducing Aldo-Keto reductase family 1 member B10 expression. *Bioengineered* 12: 1964-1975, 2021.
8. Oughtred R, Stark C, Breitkreutz BJ, Rust J, Boucher L, Chang C, Kolas N, O'Donnell L, Leung G, McAdam R, *et al*: The BioGRID interaction database: 2019 update. *Nucleic Acids Res* 47: D529-D541, 2019.
9. Komolka K, Albrecht E, Schering L, Brenmoehl J, Hoefflich A and Maak S: Locus characterization and gene expression of bovine FNDC5: Is the myokine irisin relevant in cattle? *PLoS One* 9: e88060, 2014.
10. Zhu T, Zhang W, Zhang Y, Lu E, Liu H, Liu X, Yin S and Zhang P: Irisin/FNDC5 inhibits the epithelial-mesenchymal transition of epithelial ovarian cancer cells via the PI3K/Akt pathway. *Arch Gynecol Obstet* 306: 841-850, 2022.
11. Huang CW, Chang YH, Lee HH, Wu JY, Huang JX, Chung YH, Hsu ST, Chow LP, Wei KC and Huang FT: Irisin, an exercise myokine, potently suppresses tumor proliferation, invasion, and growth in glioma. *FASEB J* 34: 9678-9693, 2020.
12. Fan GH, Zhu TY and Huang J: FNDC5 promotes paclitaxel sensitivity of non-small cell lung cancers via inhibiting MDR1. *Cell Signal* 72: 109665, 2020.
13. Cheng G, Xu D, Chu K, Cao Z, Sun X and Yang Y: The effects of MiR-214-3p and Irisin/FNDC5 on the biological behavior of osteosarcoma cells. *Cancer Biother Radiopharm* 35: 92-100, 2020.
14. Liu J, Song N, Huang Y and Chen Y: Irisin inhibits pancreatic cancer cell growth via the AMPK-mTOR pathway. *Sci Rep* 8: 15247, 2018.
15. Livak KJ and Schmittgen TD: Analysis of relative gene expression data using real-time quantitative PCR and the 2(-Delta Delta C(T)) method. *Methods* 25: 402-408, 2001.
16. Boström P, Wu J, Jedrychowski MP, Korde A, Ye L, Lo JC, Rasbach KA, Boström EA, Choi JH, Long JZ, *et al*: A PGC1- $\alpha$ -dependent myokine that drives brown-fat-like development of white fat and thermogenesis. *Nature* 481: 463-468, 2012.
17. Aydin S, Kuloglu T, Ozercan MR, Albayrak S, Aydin S, Bakal U, Yilmaz M, Kalayci M, Yardim M, Sarac M, *et al*: Irisin immunohistochemistry in gastrointestinal system cancers. *Biotech Histochem* 91: 242-250, 2016.
18. Kuloglu T, Celik O, Aydin S, Hanifi Ozercan I, Acet M, Aydin Y, Artas G, Turk A, Yardim M, Ozan G, *et al*: Irisin immunostaining characteristics of breast and ovarian cancer cells. *Cell Mol Biol (Noisy-le-grand)* 62: 40-44, 2016.
19. Kong G, Jiang Y, Sun X, Cao Z, Zhang G, Zhao Z, Zhao Y, Yu Q and Cheng G: Irisin reverses the IL-6 induced epithelial-mesenchymal transition in osteosarcoma cell migration and invasion through the STAT3/Snail signaling pathway. *Oncol Rep* 38: 2647-2656, 2017.
20. Shao L, Li H, Chen J, Song H, Zhang Y, Wu F, Wang W, Zhang W, Wang F, Li H and Tang D: Irisin suppresses the migration, proliferation, and invasion of lung cancer cells via inhibition of epithelial-to-mesenchymal transition. *Biochem Biophys Res Commun* 485: 598-605, 2017.
21. Gannon NP, Vaughan RA, Garcia-Smith R, Bisoffi M and Trujillo KA: Effects of the exercise-inducible myokine irisin on malignant and non-malignant breast epithelial cell behavior in vitro. *Int J Cancer* 136: E197-E202, 2015.
22. Altay DU, Keha EE, Karagüzel E, Mentese A, Yaman SO and Alver A: The diagnostic value of FNDC5/Irisin in renal cell cancer. *Int Braz J Urol* 44: 734-739, 2018.
23. Wozniak S, Nowinska K, Chabowski M and Dziegiel P: Significance of Irisin (FNDC5) expression in colorectal cancer. *In Vivo* 36: 180-188, 2022.
24. Cebulski K, Nowińska K, Jabłońska K, Romanowicz H, Smolnarz B, Dziegiel P and Podhorska-Okołów M: Expression of Irisin/FNDC5 in breast cancer. *Int J Mol Sci* 23: 3530, 2022.
25. Liu H, Zhao L, Wang M, Yang K, Jin Z, Zhao C and Shi G: FNDC5 causes resistance to sorafenib by activating the PI3K/Akt/Nrf2 pathway in hepatocellular carcinoma cells. *Front Oncol* 12: 852095, 2022.
26. Shao X, Wu J, Yu S, Zhou Y and Zhou C: AKR1B10 inhibits the proliferation and migration of gastric cancer via regulating epithelial-mesenchymal transition. *Aging (Albany NY)* 13: 22298-22314, 2021.
27. Yao Y, Wang X, Zhou D, Li H, Qian H, Zhang J, Jiang L, Wang B, Lin Q and Zhu X: Loss of AKR1B10 promotes colorectal cancer cells proliferation and migration via regulating FGF1-dependent pathway. *Aging (Albany NY)* 12: 13059-13075, 2020.
28. Ren P, Ren X, Cheng L and Xu L: Frankincense, pine needle and geranium essential oils suppress tumor progression through the regulation of the AMPK/mTOR pathway in breast cancer. *Oncol Rep* 39: 129-137, 2018.
29. Plews RL, Mohd Yusof A, Wang C, Saji M, Zhang X, Chen CS, Ringel MD and Phay JE: A novel dual AMPK activator/mTOR inhibitor inhibits thyroid cancer cell growth. *J Clin Endocrinol Metab* 100: E748-E756, 2015.
30. Yue W, Zheng X, Lin Y, Yang CS, Xu Q, Carpizo D, Huang H, DiPaola RS and Tan XL: Metformin combined with aspirin significantly inhibit pancreatic cancer cell growth in vitro and in vivo by suppressing anti-apoptotic proteins Mcl-1 and Bcl-2. *Oncotarget* 6: 21208-21224, 2015.



This work is licensed under a Creative Commons Attribution-NonCommercial-NoDerivatives 4.0 International (CC BY-NC-ND 4.0) License.